

Scattering processes in antiprotonic hydrogen - hydrogen atom collisions*

V.P. Popov and V.N. Pomerantsev
Institute of Nuclear Physics, Moscow State University

The elastic scattering, Stark transitions and Coulomb deexcitation of highly excited antiprotonic hydrogen atoms in collisions with hydrogen atoms have been studied in the framework of the fully quantum-mechanical close-coupling method for the first time. The total cross sections $\sigma_{nl \rightarrow n'l'}(E)$ and averaged on the initial angular momentum l cross sections $\sigma_{n \rightarrow n'}(E)$ have been calculated for the initial states of $(\bar{p}p)_n$ atoms with the principal quantum number $n = 3 - 12$ and at the relative energies $E = 0.05 - 50$ eV. The energy shifts of the ns states due to strong interaction and relativistic effects are taken into account. The results are compared with the recent semiclassical calculations.

I. INTRODUCTION

The slowing down and Coulomb capture of the negative particle M^- ($M^- = \mu^-, \pi^-, etc.$) in hydrogen media lead to the formation of the M^- -molecular complex which decay results in the exotic atom formation in highly excited states with the principal quantum number $n \sim \sqrt{\mu}$ where μ is the reduced mass of the exotic atom. Their initial nl -population and kinetic energy distribution are defined by the competition of different decay modes of this complex. The further destiny of the exotic atom depends on the kinetics of the processes occurring in the deexcitation cascade. The experimental data are mainly appropriate to the last stage of the atomic cascade, such as X-ray yields and the products of the weak or strong interaction of the exotic particle in the low angular momentum states with hydrogen isotopes.

Hadronic hydrogen atoms are of special interest among exotic atoms because they have the simplest structure and are the probe in the investigations of the various aspects of both the exotic atom physics and the elementary $\bar{p}p$ and $\bar{p}n$ interaction at zero energy.

In order to analyze the precision spectroscopy experimental data [1] the kinetic energy distribution must be taken into account. The velocity of the exotic hydrogen atom plays an important role due to effect of the Stark transitions on the L X-rays yields and the Doppler broadening of the L-lines due to preceding Coulomb deexcitation transitions. The energy release in the last process leads to an acceleration of the colliding partners. So the reliable theoretical backgrounds on the processes in highly-excited states are required for the detailed analysis of these data.

In this paper we present the first step to *ab initio* quantum-mechanical treatment of non-reactive scattering processes of the excited antiprotonic hydrogen atoms:

- elastic scattering

$$(ax)_n + (be^-)_\nu \rightarrow (ax)_n + (be^-)_\nu; \quad (1)$$

- Stark mixing

$$(ax)_{nl} + (be^-)_\nu \rightarrow (ax)_{n'l'} + (be^-)_\nu; \quad (2)$$

- Coulomb deexcitation

$$(ax)_{nl} + (be^-)_\nu \rightarrow (ax)_{n'l'} + (b^-e)_\nu. \quad (3)$$

Here $(a, b) = (p, d, t)$ are hydrogen isotopes and $x = K^-, \tilde{p}$; (n, l) are the principal and orbital quantum numbers of exotic atom and ν are the hydrogen atom quantum numbers. The processes (1) - (2) decelerate and accelerate while Coulomb deexcitation (3) accelerates the exotic atoms, influencing their quantum number and energy distributions during the cascade. The last process has attracted particular attention especially after the "hot" πp atoms with the kinetic energy up to 200 eV were found experimentally[2].

Starting from the classical paper by Leon and Bethe [3], Stark transitions has been treated in the semiclassical straight-line-trajectory approximation (see [4] and references therein). The fully quantum-mechanical treatment of the processes (1) - (2) based on the adiabatic description was given in [5-8].

*The work was supported by Russian Foundation for Basic Research, grant No 03-02-16616.

Recently [9, 10], the elastic scattering and Stark transitions (for $n = 2 - 5$) have also been studied in a close-coupling approach treating the interaction of the exotic hydrogen atom with hydrogen one in the dipole approximation with electron screening taken into account by model. As for the higher exotic atom states, the semiclassical approach [10] is used for the description of these processes.

As concerning the acceleration process (3) in antiprotonic atom, the parameterization based on the calculations in the semiclassical model [11] (see also [13]) is used for low-lying states ($n = 3 - 7$) and the calculations in the classical-trajectory Monte Carlo model [12, 13] are used for higher exotic atom states in the cascade calculations.

The main aim of this paper is to obtain the cross sections of the processes (1) for highly excited antiprotonic atom at low collision energies in the framework of the fully quantum-mechanical approach. For this purpose we use a unified treatment of elastic scattering, Stark transitions and Coulomb deexcitation within the close-coupling method. This approach has been applied previously for the study of the differential and total cross sections of the elastic scattering, Stark transitions and Coulomb deexcitation in the collisions of the excited muonic [14] and pionic [15] hydrogen atoms with the hydrogen ones. In the following section we briefly describe the close-coupling formalism. The results of the close-coupling calculations concerning the total cross sections of the processes (1) are presented and discussed in Sec. III. Finally, summary and concluding remarks are given in Sec. IV.

II. CLOSE-COUPPING APPROACH

A. Total wave function of the binary system in terms of basis states

The total wave function $\Psi(\boldsymbol{\rho}, \mathbf{r}, \mathbf{R})$ of the four-body system ($a\bar{p} + be^-$) satisfies the time independent Schrödinger equation with the Hamiltonian which after separating the center of mass motion can be written as

$$H = -\frac{1}{2m}\Delta_{\mathbf{R}} + h_{\bar{p}}(\boldsymbol{\rho}) + h_e(\mathbf{r}) + V(\mathbf{r}, \boldsymbol{\rho}, \mathbf{R}) \quad (4)$$

(m is the reduced mass of the system).

Here we use the set of Jacobi coordinates $(\mathbf{R}, \boldsymbol{\rho}, \mathbf{r})$:

$$\mathbf{R} = \mathbf{R}_H - \mathbf{R}_{\bar{p}a}, \quad \boldsymbol{\rho} = \mathbf{r}_{\bar{p}} - \mathbf{r}_a, \quad \mathbf{r} = \mathbf{r}_e - \mathbf{r}_b,$$

where $\mathbf{r}_a, \mathbf{r}_b, \mathbf{r}_{\bar{p}}, \mathbf{r}_e$ are the radius-vectors of the nuclei, muon and electron in the lab-system, $\mathbf{R}_H, \mathbf{R}_{\bar{p}a}$ are the center of mass radius-vectors of the hydrogen and exotic atoms, respectively. The Hamiltonians $h_{\bar{p}}$ and h_e of the free exotic and hydrogen atoms, respectively, satisfy the Schrödinger equations

$$h_{\mu}\Phi_{nlm}(\boldsymbol{\rho}) = \varepsilon_{nl}\Phi_{nlm}(\boldsymbol{\rho}), \quad (5)$$

$$h_e\varphi_{n_e l_e}(\mathbf{r}) = \epsilon_{n_e}\varphi_{n_e l_e}(\mathbf{r}), \quad (6)$$

where $\Phi_{nlm}(\boldsymbol{\rho})$ and $\varphi_{n_e}(\mathbf{r})$ are the hydrogen-like wave functions of the exotic atom and hydrogen atom bound states, ε_{nl} and ϵ_{n_e} are the corresponding eigenvalues. In the present study the ε_{nl} includes beyond the standard non-relativistic two-body Coulomb problem the energy shifts due to strong interaction, vacuum polarization and finite size. It is noting that in order to treat the hadronic ns states as normal asymptotic states in the scattering problem we take into consideration only the real part of the complex strong interaction energy shift.

The interaction potential

$$V(\mathbf{r}, \boldsymbol{\rho}, \mathbf{R}) = V_{ab} + V_{\mu b} + V_{ae} + V_{\mu e} \quad (7)$$

includes the pair Coulomb interactions between the particles from two colliding subsystem:

$$V_{ab} = \frac{1}{r_{ab}} = |\mathbf{R} + \nu\boldsymbol{\rho} - \nu_e\mathbf{r}|^{-1}, \quad V_{\bar{p}b} = -\frac{1}{r_{\bar{p}b}} = -|\mathbf{R} - \xi\boldsymbol{\rho} - \nu_e\mathbf{r}|^{-1}, \quad (8)$$

$$V_{\bar{p}e} = \frac{1}{r_{\bar{p}e}} = |\mathbf{R} - \xi\boldsymbol{\rho} + \xi_e\mathbf{r}|^{-1}, \quad V_{ae} = -\frac{1}{r_{ae}} = -|\mathbf{R} + \nu\boldsymbol{\rho} + \xi_e\mathbf{r}|^{-1}, \quad (9)$$

where the following notations are used:

$$\nu = m_{\bar{p}}/(m_{\bar{p}} + m_a), \quad \xi = m_a/(m_{\bar{p}} + m_a), \quad (10)$$

$$\nu_e = m_e/(m_e + m_b), \quad \xi_e = m_b/(m_e + m_b), \quad (11)$$

($m_a, m_b, m_{\bar{p}}$ and m_e are the masses of the hydrogen isotopes, antiproton and electron, respectively). Atomic units (a.u) $\hbar = e = m_e m_b / (m_e + m_b) = 1$ will be used throughout the paper unless otherwise stated.

In this paper, as well as in the previous studies [11, 12-15], we assume that the state of the target electron is fixed during the collision. The electron excitations can be taken into account in a straightforward manner. In a space-fixed coordinate frame we built the basis states from the eigenvectors of the operators $h_e, h_{\bar{p}}, \mathbf{I}^2, \mathbf{L}^2, \mathbf{J}^2, J_z$ and the total parity π with the corresponding eigenvalues $\varepsilon_{1s}, \varepsilon_n, l(l+1), L(L+1), J(J+1), M$ and $(-1)^{l+L}$, respectively:

$$|1s, nl, L : JM\rangle \equiv \frac{1}{\sqrt{4\pi}} R_{1s}(r) R_{nl}(\rho) \mathcal{Y}_{lL}^{JM}(\hat{\boldsymbol{\rho}}, \hat{\mathbf{R}}), \quad (12)$$

where

$$\mathcal{Y}_{lL}^{JM}(\hat{\boldsymbol{\rho}}, \hat{\mathbf{R}}) \equiv \sum_{m\lambda} \langle lmL\lambda | JM \rangle Y_{lm}(\hat{\boldsymbol{\rho}}) Y_{L\lambda}(\hat{\mathbf{R}}). \quad (13)$$

Here the orbital angular momentum \mathbf{l} of $(a\mu)_{nl}$ is coupled with the orbital momentum \mathbf{L} of the relative motion to give the total angular momentum, $\mathbf{J} = \mathbf{l} + \mathbf{L}$. The explicit form of the radial hydrogen-like wave functions $R_{nl}(\rho)$ will be given below.

Then, for the fixed values of $J, M, \pi = (-1)^{l+L}$ the exact solution of the Schrödinger equation

$$(E - H) \Psi_E^{JM\pi}(\mathbf{r}, \boldsymbol{\rho}, \mathbf{R}) = 0, \quad (14)$$

is expanded as follows

$$\Psi_E^{JM\pi}(\mathbf{r}, \boldsymbol{\rho}, \mathbf{R}) = \frac{1}{R} \sum_{nlL} G_{nlL}^{J\pi}(R) |1s, nl, L : JM\rangle, \quad (15)$$

where the $G_{nlL}^{J\pi}(R)$ are the radial functions of the relative motion and the sum is restricted by the (l, L) values to satisfy the total parity conservation. This expansion leads to the coupled radial scattering equations

$$\left(\frac{d^2}{dR^2} + k_n^2 - \frac{L(L+1)}{R^2} \right) G_{nlL}^{J\pi}(R) = 2m \sum_{n'l'L'} W_{n'l'L',nlL}^J(R) G_{n'l'L'}^{J\pi}(R), \quad (16)$$

where $k_{nl}^2 = 2m(E_{cm} + \varepsilon_{n_i l_i} - \varepsilon_{nl})$ specifies the channel wave numbers; E_{cm} and $\varepsilon_{n_i l_i}$ are the relative motion energy and bound energy of exotic atom in the entrance channel.

The radial functions $G_{E,nlL}^{J\pi}(R)$ satisfy the usual plane-wave boundary conditions at $R \rightarrow 0$

$$G_{E,n'l'L'}^{J\pi}(0) = 0 (\sim R^{L+1}) \quad (17)$$

and at asymptotic distances ($R \rightarrow \infty$)

$$G_{E,n'l'L'}^{J\pi}(R) \Rightarrow \frac{1}{\sqrt{k_f}} \{ \delta_{if} \delta_{nn'} \delta_{ll'} \delta_{LL'} e^{-i(k_i R - L\pi/2)} - S^J(nl, L \rightarrow n'l', L') e^{i(k_f R - L'\pi/2)} \}, \quad (18)$$

where k_i, k_f are the wave numbers of initial and final channels and $S^J(nl, L \rightarrow n'l', L')$ is the scattering matrix in the total angular momentum representation. Here and below the indices of the entrance channel and target electron state are omitted for brevity.

B. Potential matrix

Here we present the derivation of the exact matrix of the interaction potentials involved in the close-coupling calculations. The interaction potential matrix $W_{n'l'L',nlL}^J$ coupling the asymptotic initial $(nlL; J)$ and final $(n'l'L'; J)$ channels is defined by

$$W_{n'l'L, n'lL}^J(R) = \frac{1}{4\pi} \int d\mathbf{r} d\boldsymbol{\rho} d\hat{\mathbf{R}} R_{1s}^2(r) R_{nl}(\rho) R_{n'l'}(\rho) \times \mathcal{Y}_{lL}^{JM}(\hat{\boldsymbol{\rho}}, \hat{\mathbf{R}}) V(\mathbf{r}, \boldsymbol{\rho}, \mathbf{R})' (\mathcal{Y}_{l'L'}^{JM})^*(\hat{\boldsymbol{\rho}}, \hat{\mathbf{R}}), \quad (19)$$

where the radial hydrogen-like wave functions are given explicitly by

$$R_{nl}(\rho) = N_{nl} \left(\frac{2\rho}{na} \right)^l \exp(-\rho/na) \sum_{q=0}^{n-l-1} S_q(n, l) \left(\frac{2\rho}{na} \right)^q \quad (20)$$

(a is the Bohr' radius of the exotic atom in a.u.) with

$$N_{nl} = \left(\frac{2}{na} \right)^{3/2} \left[\frac{(n+l)!(n-l-1)!}{2n} \right]^{1/2}, \quad (21)$$

$$S_q(n, l) = (-)^q \frac{1}{q!(n-l-1-q)!(2l+1+q)!}. \quad (22)$$

Averaging $V(\mathbf{r}, \boldsymbol{\rho}, \mathbf{R})$ over 1s-state of hydrogen atom leads to

$$\begin{aligned} V(\mathbf{R}, \boldsymbol{\rho}) &= \frac{1}{4\pi} \int_0^\infty d\mathbf{r} R_{1s}^2(r) V(\mathbf{r}, \boldsymbol{\rho}, \mathbf{R}) = \\ &= \frac{1}{\xi_e} \{U_{\nu, \xi_e}(\mathbf{R}, \boldsymbol{\rho}) - U_{-\xi, \xi_e}(\mathbf{R}, \boldsymbol{\rho})\} - \frac{1}{\nu_e} \{U_{\nu, \nu_e}(\mathbf{R}, \boldsymbol{\rho}) - U_{-\xi, \xi_e}(\mathbf{R}, \boldsymbol{\rho})\}. \end{aligned} \quad (23)$$

Then we use the transformation

$$U_{\alpha, \beta}(\mathbf{R}, \boldsymbol{\rho}) = \left(1 + \frac{\beta}{|\mathbf{R} + \alpha\boldsymbol{\rho}|} \right) e^{-\frac{2|\mathbf{R} + \alpha\boldsymbol{\rho}|}{\beta}} \equiv \lim_{x \rightarrow 1} \left(1 - \frac{1}{2} \frac{\partial}{\partial x} \right) \beta \frac{e^{-\frac{2x|\mathbf{R} + \alpha\boldsymbol{\rho}|}{\beta}}}{|\mathbf{R} + \alpha\boldsymbol{\rho}|}. \quad (24)$$

which allows us to apply the additional theorem for the spherical Bessel functions [16]

$$\begin{aligned} \frac{e^{-\lambda|\mathbf{R}_1 + \mathbf{r}_1|}}{|\mathbf{R}_1 + \mathbf{r}_1|} &= \frac{4\pi}{\sqrt{R_1 r_1}} \sum_{t\tau} (-1)^t Y_{t\tau}^*(\hat{\mathbf{R}}_1) Y_{t\tau}(\hat{\mathbf{r}}_1) \times \\ &\times \left\{ K_{t+1/2}(\lambda R_1) I_{t+1/2}(\lambda r_1) \Big|_{r_1 < R_1} + I_{t+1/2}(\lambda R_1) K_{t+1/2}(\lambda r_1) \Big|_{r_1 > R_1} \right\} \end{aligned} \quad (25)$$

($I_p(x)$ and $K_p(x)$ are the modified spherical Bessel functions of the first and third kind). Furthermore, after substituting of the Eqs.(24-26) into (20) we can integrate over the angular variables $(\mathbf{R}, \boldsymbol{\rho})$. Finally, applying the angular momentum algebra and integrating over ρ , we obtain:

$$\begin{aligned} W_{n'lL, n'l'L}^J(R) &= (-1)^{J+l+l'} i^{l'+L-l-L} \sqrt{\hat{l}' \hat{L} \hat{L}'} \sum_{t=0}^{t_m} (t0l'0|t0)(L0L'0|t0) \left\{ \begin{matrix} l & l' & t \\ L' & L & J \end{matrix} \right\} \times \\ &\times \left\{ \frac{1}{\xi_e} [(-1)^t W_t(R, \nu, \xi_e; nl, n'l') - W_t(R, \xi, \xi_e; nl, n'l')] - \right. \\ &\left. - \frac{1}{\nu_e} [(-1)^t W_t(R, \nu, \nu_e; nl, n'l') - W_t(R, \xi, \nu_e; nl, n'l')] \right\} \end{aligned} \quad (26)$$

(t_m is the maximum value of the allowed multipoles). Here the next notations are used:

$$\begin{aligned} W_t(R, \alpha, \beta; nl, n'l') &= \mathcal{N}_{nl, n'l'} \sum_{m_1=0}^{n-l-1} S_{m_1}(n, l) \left(\frac{2n'}{n+n'} \right)^{m_1} \sum_{m_2=0}^{n'-l'-1} S_{m_2}(n', l') \left(\frac{2n}{n+n'} \right)^{m_2} \times \\ &\times \left\{ H_t(x) J_1^{t,s}(x, \lambda(n, n', \alpha, \beta)) - h_t(x) J_2^{t,s}(x, \lambda(n, n', \alpha, \beta)) + \right. \\ &\left. + F_t(x) J_3^{t,s}(x, \lambda(n, n', \alpha, \beta)) + f_t(x) J_4^{t,s}(x, \lambda(n, n', \alpha, \beta)) \right\}, \end{aligned} \quad (27)$$

where $x = 2R/\beta$, $s = l + l' + m_1 + m_2$, $\hat{L} \equiv 2L + 1$;

$$\mathcal{N}_{nl,n'l'} = \frac{1}{n+n'} \left(\frac{2n'}{n+n'} \right)^{l+1} \left(\frac{2n}{n+n'} \right)^{l'+1} \sqrt{(n+l)!(n-l-1)!(n'+l)!(n'-l'-1)}; \quad (28)$$

$$\lambda(n, n', \alpha, \beta) = \frac{2nn'}{n+n'} \frac{a\alpha}{\beta}; \quad (29)$$

$$H_t(x) = (1 - 2t)h_t(x) + xh_{t+1}(x); \quad (30)$$

$$F_t(x) = (1 - 2t)f_t(x) - xf_{t+1}(x). \quad (31)$$

The functions $h_t(x)$ and $f_t(x)$ are given by

$$h_t(x) \equiv \sqrt{\frac{2}{\pi x}} K_{t+1/2}(x) \quad (32)$$

and

$$f_t(x) \equiv \sqrt{\frac{\pi}{2x}} I_{t+1/2}(x). \quad (33)$$

The radial integrals $J_i^{t,s}(x, \lambda)$ are defined as follows:

$$J_1^{t,s}(x, \lambda) = \int_0^{x/\lambda} y^{s+2} e^{-y} f_t(\lambda y) dy, \quad (34)$$

$$J_2^{t,s}(x, \lambda) = \lambda J_1^{t+1, s+1}(x, \lambda), \quad (35)$$

$$J_3^{t,s}(x, \lambda) = \int_{x/\lambda}^{\infty} y^{s+2} e^{-y} h_t(\lambda y) dy, \quad (36)$$

$$J_4^{t,s}(x, \lambda) = \lambda J_3^{t+1, s+1}(x, \lambda) \quad (37)$$

and calculated analytically using the power series for the modified Bessel functions.

C. Cross sections

The transition amplitude from the initial state $|nlm\rangle$ to the final state $|n'l'm'\rangle$ of exotic atom can be defined by

$$\begin{aligned} f(nlm \rightarrow n'l'm' | \mathbf{k}_i, \mathbf{k}_f) &= \frac{2\pi i}{\sqrt{k_i k_f}} \sum_{JM L L' \lambda \lambda'} i^{L'-L} \langle l m L \lambda | JM \rangle \langle l' m' L' \lambda' | JM \rangle \times \\ &\times Y_{L\lambda}^*(\hat{\mathbf{k}}_i) Y_{L'\lambda'}(\hat{\mathbf{k}}_f) T^J(nlL \rightarrow n'l'L'). \end{aligned} \quad (38)$$

Here, k_i and k_f are the cms relative momenta in the initial and final channels; $\hat{\mathbf{k}}_i$ and $\hat{\mathbf{k}}_f$ are their unit vectors in the space-fixed system, respectively, and, finally, the transition matrix $T^J(nlL \rightarrow n'l'L')$ used here is given by

$$T^J(nl, L \rightarrow n'l', L') = \delta_{nn'} \delta_{ll'} \delta_{LL'} \delta_{mm'} \delta_{\lambda\lambda'} - S^J(nl, L \rightarrow n'l', L'). \quad (39)$$

In terms of the scattering amplitude defined above, all the types both the differential and total cross sections of all processes under consideration for the transition from the initial (nl) state to the final ($n'l'$) state are defined as:

differential cross sections

$$\frac{d\sigma_{nl \rightarrow n'l'}}{d\Omega} = \frac{1}{2l+1} \frac{k_f}{k_i} \sum_{mm'} |f(nlm \rightarrow n'l'm' | \mathbf{k}_i, \mathbf{k}_f)|^2, \quad (40)$$

partial cross sections

$$\sigma_{nl \rightarrow n'l'}^J(E) = \frac{\pi}{k_i^2} \frac{2J+1}{2l+1} \sum_{LL'} |T^J(nlL \rightarrow n'l'L')|^2, \quad (41)$$

and the total cross sections for the $nl \rightarrow n'l'$ transition is obtained by summing the corresponding partial cross section over the total angular momentum J :

$$\sigma_{nl \rightarrow n'l'}(E) = \sum_J \sigma_{nl \rightarrow n'l'}^J(E). \quad (42)$$

Finally, the averaged over the initial orbital angular momentum l -averaged cross sections for the $n \rightarrow n'$ transitions are then defined by summing over l' and l ($l = l'$ for elastic scattering and $l \neq l'$ for Stark transitions) with the statistical weight $(2l+1)/n^2$ in a case of the degenerated exotic atom states and with the weight $(2l+1)/(n^2-1)$ in the case when the energy shift of the ns state is taken into account:

$$\sigma_{n \rightarrow n'}^{av}(E) = \frac{\pi}{k_i^2} \sum_{l, l', LL', J} \frac{2J+1}{n^2} |T^J(nlL \rightarrow n'l'L')|^2, \quad (43)$$

and

$$\sigma_{n \rightarrow n'}^{l>0}(E) = \frac{\pi}{k_i^2} \sum_{l, l', LL', J} \frac{2J+1}{n^2-1} |T^J(nlL \rightarrow n'l'L')|^2, \quad (44)$$

respectively.

III. RESULTS

The close-coupling method described in the previous Section has been used to obtain the total cross sections for the collisions of the $\bar{p}p$ atoms in excited states with hydrogen atoms. The present calculations had at least two goals: first, to apply the fully quantum-mechanical approach for the study of the processes (1) - (3) and, second, to clear the effect of the energy shifts of the ns states of the antiprotonic hydrogen atom on the cross sections of these processes.

The coupled differential equations are solved numerically by the Numerov method with the standing-wave boundary conditions involving the real K -matrix. The corresponding T -matrix are obtained from K -matrix using the matrix equation $T = 2iK(I - iK)^{-1}$. In the calculations we have taken into account the exact interaction matrix and all open channels with $n' \leq n$. The closed channels are not considered in the present paper. The close-coupling calculations have been carried out for the relative collision energies E_{cm} from 0.05 up to 50 eV and for the excited states with $n = 3 \div 12$. At all energies the convergence of the partial wave expansion was reached and all cross sections were calculated with the accuracy better than 0.1%.

The results of the calculations are presented in Figures 1-4. In Fig. 1 we present the calculated total cross sections of $nl \rightarrow n'l'$ transitions for $n = 8$ at kinetic energy $E_{cm} = 1.4$ eV both with and without energy shift of ns state. The following measured world -average value [17] for the spin-averaged shift was used in the present calculations

$$\epsilon_{1s} = 721 \pm 14 \text{eV (repulsive)}.$$

and the energy shifts of the ns states are defined by ϵ_{1s}/n^3 .

The energy shift of the ns states in $\bar{p}p$ atom is repulsive, hence the $nl \rightarrow ns$ transitions are closed below the corresponding threshold and according with the present study (e.g., see Fig. 1) the Stark transitions

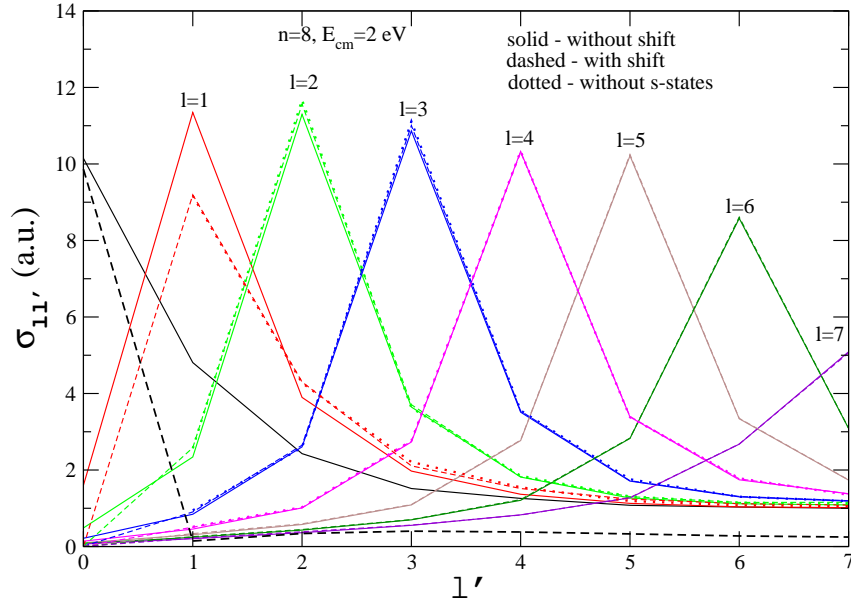


FIG. 1: The total cross sections $\sigma_{n_l \rightarrow n_{l'}}$ for collisions $p\bar{p}$ atom in the $n = 8$ state with hydrogen atom at $E_{r_{mcm}} = 1.4$ eV. The points corresponding the calculations with and without taking into account for the shifts ns -states are connected with dashed and solid lines, respectively. The results obtained without including all s -state are designated with dotted lines.

both from ns state and to ns state are strongly suppressed at the kinetic energies above the threshold. The similar effect is also observed for the elastic $np \rightarrow np$ transitions. The other transitions are practically unchangeable at fixed energy. The analog of this effect can be modeled by the excluding the ns state from the basis states. At energy above a few thresholds the effect is much weaker. Therefore, the strong interaction effect in antiprotonic hydrogen (the similar effect must be observed in kaonic hydrogen atom) results in the essential and important difference of the Stark transition role in the absorption from ns states in contrast with the pionic hydrogen atoms. The influence of the strong interaction shift enhances for lower states and becomes less pronounced for highly excited states of the antiprotonic atom.

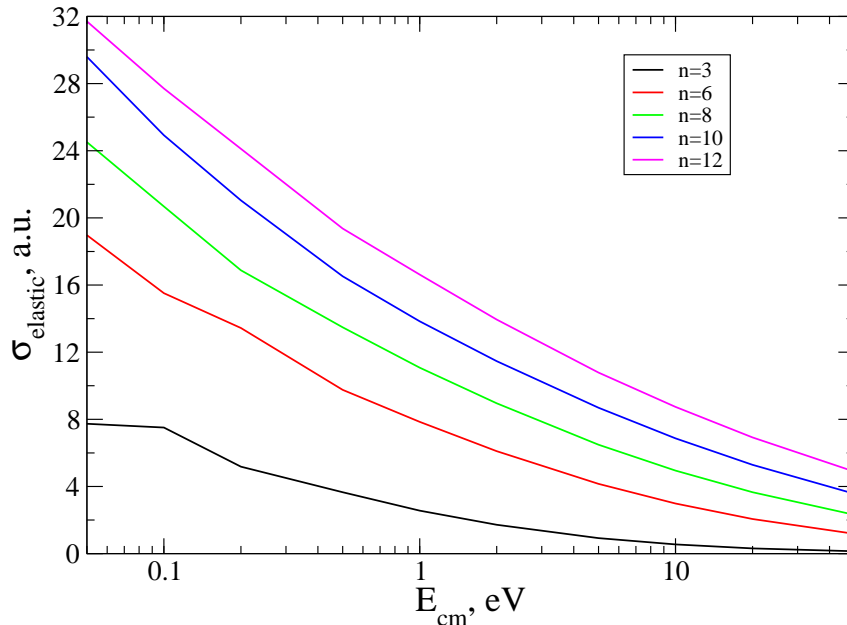


FIG. 2: The l -averaged cross sections of elastic scattering for collisions $p\bar{p}$ atom with hydrogen atom

In Figures 2 and 3 the energy dependence of the l -averaged total elastic and Stark cross sections are

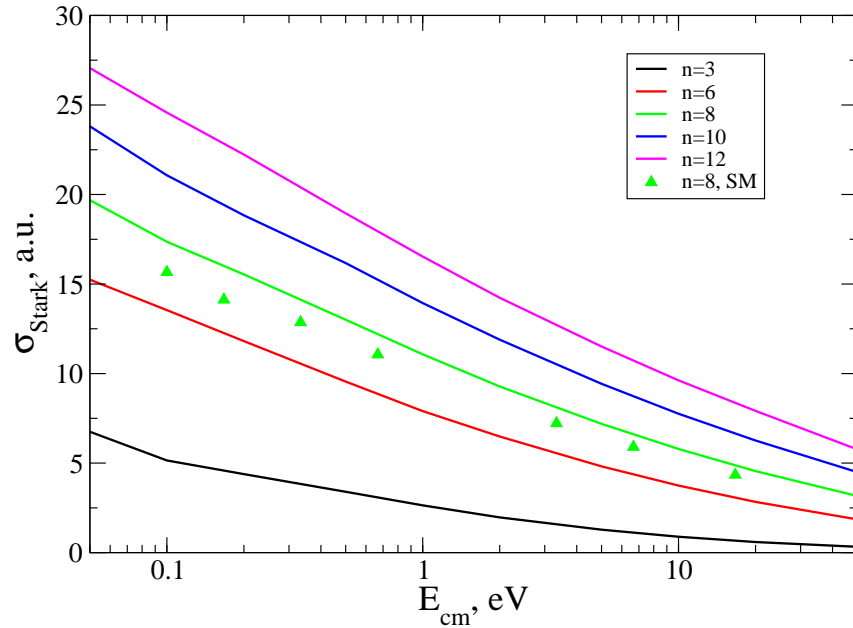


FIG. 3: The l -averaged cross sections of Stark transitions for collisions $p\bar{p}$ atom with hydrogen atom. The results of previous semiclassical calculations [12] are shown for $n = 8$ with triangles

shown for different values of the principle quantum number n . Since the relative contribution of the ns state in the l -averaged cross sections are small, the calculations both with and without the energy shift are practically indistinguishable at the energies above the corresponding threshold. So, in Figs. 2 and 3 the small energy region corresponds to the calculations without energy shift taken into account. In Fig. 3 the l -averaged cross section for $n=8$ are compared with the calculations in the framework of the semiclassical model [10]. As a whole a fair agreement is observed, but the semiclassical model results in a slightly different energy dependence especially at low energy collision.

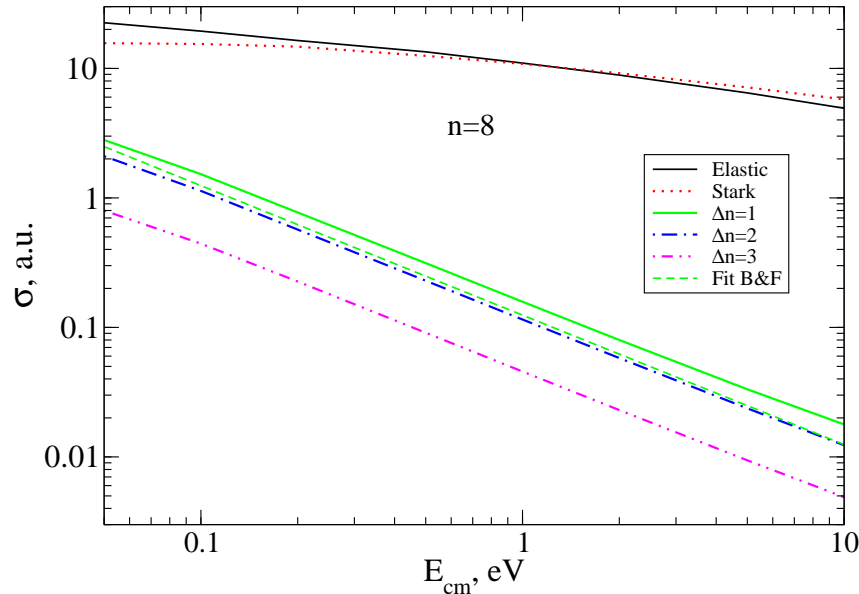


FIG. 4: The l -averaged cross sections of Coulomb deexcitation with $\Delta n = 1, 2, 3$ for collisions $p\bar{p}$ atom in the $n = 8$ state with hydrogen atom. The dashed line shows the fit used in cascade calculations [13] and based on results of [11]

The dependence of the Coulomb deexcitation cross sections on energy is illustrated in Fig. 4 for $n = 8$ and different values of $\Delta n = 1, 2$ and 3. The special features of these cross sections are: the similar energy

dependence but sharper than that of the elastic scattering and Stark transitions (see also in Fig. 4); the contribution of the transitions with $\Delta n > 1$ is comparable with the one for $\Delta n = 1$ and approximately equal about 50%. The effect of the energy shift of the ns states in l -averaged Coulomb deexcitation cross sections are small for the same reason as discussed above. In Fig. 4 we also compare our results with the those obtained in the semiclassical model (we use the parameterization suggested in [13] which gives a fair description of the Coulomb cross sections from [11]) for $\Delta n = 1$ transition. The satisfactory agreement is observed, but this agreement is quite occasional and have no place for other n values. The distribution over the final states n' is completely different from the semiclassical results [11] as illustrated in Fig. 4. The present calculations predict that $\Delta n > 1$ transitions give a substantial contribution in the Coulomb deexcitation of highly excited exotic atom that is in agreement with our previous results for muonic and pionic hydrogen [14,15].

IV. CONCLUSION

The unified treatment of the elastic scattering, Stark transitions and Coulomb deexcitation is presented in *ab initio* quantum-mechanical approach and for the first time the cross sections of these processes are calculated for the highly excited antiprotonic hydrogen atom. The influence of the energy shifts of the ns states on these processes are studied. We have found that the strong interaction shifts in antiprotonic hydrogen atom lead to substantial suppression both $ns \rightarrow nl' \neq 0$ and $nl' \neq 0 \rightarrow ns$ transitions. At the same time, the other transitions are practically unchangeable. Our study is the first step to achievement a reliable theoretical input for the realistic kinetics calculations.

We are grateful to Prof. L.Ponomarev for the stimulating interest and support of this investigation.

-
- [1] D. Gotta et al., Newsletter **15**, 276 (1999).
 - [2] J.F.Crawford et al., Phys.Rev. D **43**, 46
 - [3] M.Leon and H.A.Bethe, Phys.Rev. **127**, 636 (1962).
 - [4] T.P.Terrado and R.S. Hayano, Phys.Rev. C **55**, 73, (1977).
 - [5] V.P.Popov and V.N.Pomerantsev, Hyp. Interact. **101/102**, 133 (1996).
 - [6] V.P.Popov and V.N.Pomerantsev, Hyp. Interact. **119**, 133 (1999).
 - [7] V.P.Popov and V.N.Pomerantsev, Hyp. Interact. **119**, 137 (1999).
 - [8] V.V.Gusev, V.P.Popov and V.N.Pomerantsev, Hyp. Interact. **119**, 141 (1996).
 - [9] T.S.Jensen and V.E.Markushin, PSI-PR-99-32 (1999); nucl-th/0001009.
 - [10] T.S.Jensen and V.E.Markushin, Eur.Journ.Phys. D, **19**, 165 (2001).
 - [11] L.Bracci and G.Fiorentini, Nuovo Cim. **43A**, 9 (1978).
 - [12] T.S.Jensen and V.E.Markushin, physics/0205076.
 - [13] T.S.Jensen and V.E.Markushin, physics/0205077.
 - [14] G.Ya. Korenman, V.N. Pomerantsev, and V.P. Popov, JETP Lett. **81**, 543 (2005); nucl-th/0501036.
 - [15] V.N. Pomerantsev and V.P. Popov, nucl-th/0511026.
 - [16] Handbook of mathematical functions, eds. M. Abramowitz and I.A. Stegun, National Bureau of Standards, Applied mathematical series - 55, 1964.
 - [17] M.Augsburger et al., Nucl. Phys. A **658**, 149 (1999)